

# Thermal Characteristics of Microswitch Contacts

Xiaomin Yan, N. E. McGruer, G. G. Adams\*, S. Majumder\*\*,

Electrical Engineering Department,

\* Mechanical Engineering Department,

Northeastern University, Boston, MA 02115

\*\*Analog Devices, Wilmington, MA 01887

**Abstract** -- Electrostatically actuated microswitches and relays have been developed at Northeastern University. These devices are approximately 100 x 100 microns in size and have been tested up to  $10^{10}$  cycles with a current of 2 mA per contact. In this paper we examine the thermal characteristics of a microswitch with Au-Au contacts. We describe a finite element model to study the temperature distribution in the microswitch. The modeling results show that the highest temperature is located in the thin film contact trace rather than at the contact interface. The hottest spot moves away from the contact as the contact radius increases. Measurements show the switch resistance increases with voltage. The contact trace melts at a switch current of 0.35 A per contact and a voltage of 0.45 V. The melted region is 3-5  $\mu\text{m}$  away from the center of the contact, slightly further than is predicted by the model.

## I. INTRODUCTION

Electrostatically actuated micromechanical switches have been developed at Northeastern University, using the NUMEM microfabrication process [1]. Fig. 1 is a schematic representation of a microswitch, and Fig. 2 shows a SEM micrograph of a fabricated device. The microswitch design is based on a double cantilever beam, and has 3 electrical terminals, labeled source, gate and drain in Figs. 1 and 2. These switches can be used in RF and microwave circuits, medical ultrasound systems and ATE systems.

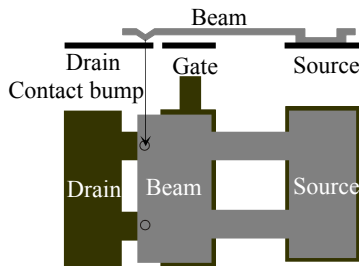


Fig. 1. Schematic of a microswitch.

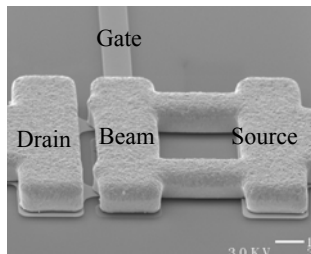


Fig. 2. SEM micrograph of a microswitch.

Applying a voltage between the gate and source terminals creates an electrostatic force between the gate electrode and

the cantilever, and pulls the beam down to make electrical contact with the drain. The minimum actuating gate-to-source voltage required to close a microswitch is typically 20-60 V, depending on the device geometry. This is referred to as the threshold voltage.

When the microswitch closes, contact between the beam and the drain electrode occurs through a pair of bumps on the lower surface of the beam, near its free end. Fig. 3 shows a micrograph of a contact bump on the bottom of a beam.

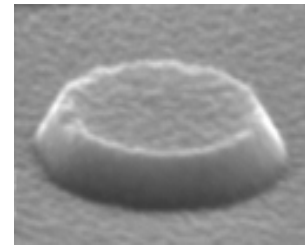


Fig. 3. Micrograph of a contact bump on a microswitch. The radius of the contact bump is 1  $\mu\text{m}$  and its height is 0.3  $\mu\text{m}$ .

Analysis and measurements of our microswitches have been reported earlier [2][3]. Switches have been cycled in excess of  $10^{10}$  cycles with a current of 2 mA per contact. Testing is done in a nitrogen ambient at atmospheric pressure, with current being applied to the contacts during each cycle only when the switch is closed. Switches with Au-Au contacts typically have contact resistances less than 1  $\Omega$ .

Microswitches with 2 contact bumps have a shortened lifetime at higher currents. For gold-gold contacts, the microswitches fail in a permanently closed mode at less than 1000 cycles for currents exceeding 20 mA, and at less than 10 cycles for currents exceeding 300 mA. At currents of approximately 1 A, the drain electrode melts, resulting in a permanently open switch.

To understand and improve the current handling capability of the microswitches, we need to study their thermal

characteristics. Many authors have reported on various aspects of heat conduction through a contact (e.g., [4,5,6,7,8]). There is also a large body of work on the thermal modeling of macroscopic relay contacts, using finite element and finite difference methods (e. g., [9, 10]). Hyman has discussed the contact physics of microcontacts, and modeled their thermal behaviour [11]. However, he does not consider the effect of the thin film traces leading up to the contacts in most MEMS switch designs.

In this paper, recent work on the thermal characteristics of our microswitches is presented. First, the general contact theory is reviewed in Section II. In Section III, the results of an idealized finite element model in ANSYS are compared to analytical results to show that the finite element model is reasonable. In Section IV, the finite element model of our microswitches is described, and simulation results are discussed. In Section V, some experimental results are reported and compared to the modeling results. Our work is summarized in Section VI.

## II. CONTACT THEORY

### A. Contact Resistance

Assuming that the electrical resistivity,  $\rho$ , is the same at all points of the constriction, the contact resistance of a single spot separating two infinite hemispheres is [12]:

$$R = \frac{\rho}{2a} . \quad (1)$$

where  $a$  is the radius of the contact spot.

Because of the roughness of a real contact surface, only a few asperities of different radii, or at most tens of asperities, will make contact. Majumder et al. [13] have modeled the contact resistance of multiple contact spots in our microswitches, based on contact mechanics literature [14, 15].

In the following discussion, we represent the contact spots by an effective single spot, whose area is equal to the total area of all the individual contact spots combined. Based on SEM micrographs of the contact and electrical measurements, we assume an effective contact radius of about  $0.1 \mu m$ .

### B. Voltage-Temperature Relation

There is a simple relation between the voltage and the temperature difference across a contact. It is a consequence of the Wiedemann-Franz law [12] that relates the electrical resistivity to the thermal conductivity. This relation is often called the  $\varphi$ - $\theta$  Relation [12]

$$L(T_\theta^2 - T_0^2) = U^2 / 4 , \quad (2)$$

where,  $T_\theta$  is the maximum temperature in a constriction,  $T_0$  is the reference temperature and  $U$  is the voltage across the constriction. The parameter  $L$  is approximately:

$$L = 2.4 \cdot 10^{-8} (V/K)^2 \quad (3)$$

If  $T_\theta$  is room temperature (300K) and  $T_\theta$  is the softening, melting or boiling temperature of a metal, then  $U_s$ ,  $U_m$  and  $U_{bl}$  are the corresponding voltages defined by (2). These voltages are called the softening, melting and boiling voltages respectively. They can often be observed by critical changes of the contact resistance [12]. For bulk gold, the softening, melting and boiling temperatures are 373 K, 1336 K, and 2720 K, and the corresponding voltages are 0.07 V, 0.4 V, and 0.95 V.

Although the relation is derived for symmetric contacts, non-symmetric contacts usually show only small differences in the paths of the electric and thermal currents, and the relation can be applied to them without a large error. However, several workers have reported deviations from (2) [16, 17].

## III. FINITE ELEMENT ANALYSIS (FEA) OF AN IDEALIZED MODEL

First, the flow of current through a contact spot separating two hemispheres is modeled using the finite element software ANSYS. This is done to verify that the FEA model gives accurate results, and also to study the behavior of an idealized contact, before we model the contact more realistically.

### A. Description of the Idealized Model

Two hemispheres contact at a spot, whose radius is  $a$ . Because of the axisymmetry of the model, it can be simplified into a 2-d model in ANSYS. The contact is a line of length  $a$  shared by two quarters of a circle, which represent the two hemispheres (Fig. 4).

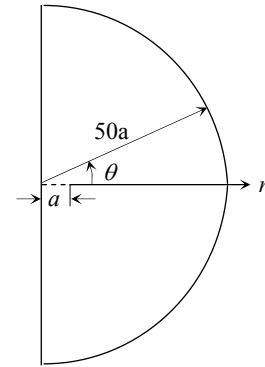


Fig. 4. Schematic of axisymmetric model in ANSYS.

The boundary conditions are:

$$\begin{aligned} T &= 300K && \text{at } r = 50a , \\ h_f &= 0 && \text{at } a < r < 50a , \theta = 0 , \\ U &= V_{load} && \text{at } r = 50a , 0^\circ \leq \theta \leq 90^\circ , \\ U &= 0 && \text{at } r = 50a , -90^\circ \leq \theta < 0^\circ . \end{aligned}$$

where  $h_f$  denotes heat flux,  $T$  denotes temperature, and  $U$  denotes voltage.

### B. Contact Resistance of the Idealized Model

The constriction resistance was calculated for a number of finite element analyses with different mesh granularities. The material properties used were those of bulk Au at room temperature, as reported in [18]. According to (1), the theoretical resistance is 11.21 m $\Omega$ . The contact resistance approaches the theoretical value as the number of model elements increases from 18600 to 34000. The number of nodes along the 1  $\mu\text{m}$  contact radius increases from 3 to 180. The error is less than 1% as long as the number of elements is more than 25000.

### C. Voltage Temperature Relation

When a voltage,  $V_{\text{load}}$ , is applied between the two outer surfaces of the hemispheres, a current flows through the constriction and heat is generated. Several simulations were performed with different values of  $V_{\text{load}}$ . The temperature variation of the material parameters - thermal and electrical conductivity, density, and specific heat capacity - was as reported for bulk Au [18].

Fig. 5 shows the voltage distribution along the vertical axis passing through the center of the contact spot. It shows that most of the voltage drop occurs near the contact spot, where the constriction is located. Similarly, the maximum temperature is located at the contact spot, which is consistent with the symmetry of the model.

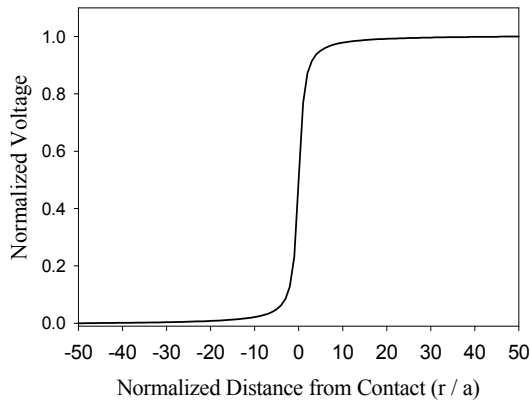


Fig. 5. Normalized voltage distribution ( $a = 1 \mu\text{m}$ ).

With increasing  $V_{\text{load}}$ , the temperature increases everywhere correspondingly. Fig. 6 shows the change in the maximum temperature with  $V_{\text{load}}$ . For comparison, the theoretical temperature-voltage relation, (2), is shown. The relation obtained from FEA is consistent with the analytical equation when the temperature is low. At a high  $V_{\text{load}}$ , the FEA result deviates from (2). That is because the material

parameters used in FEA are experimental values and do not follow the Wiedemann-Franz law at higher temperatures.

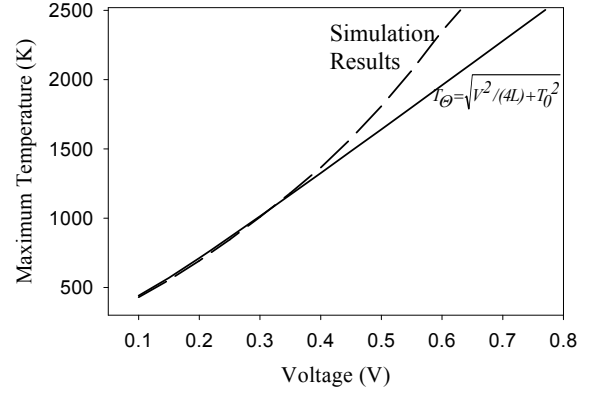


Fig. 6. Maximum temperature vs. applied voltage ( $a = 1 \mu\text{m}$ ).

## IV. FINITE ELEMENT ANALYSIS OF MICROSWITCHES

### A. Description of Model

A close-up of the microswitch contact region is shown in Fig. 7. The thin dark line is the contact bump. Figs. 8 and 9 are schematics of the region around the contact and the top view of the drain.

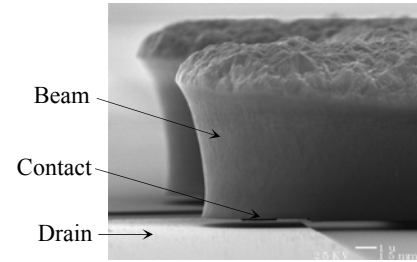


Fig. 7. Micrograph of the beam tip.

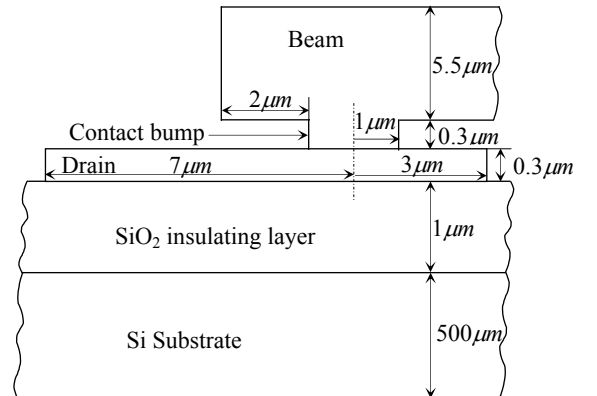


Fig. 8. Geometry of a microswitch

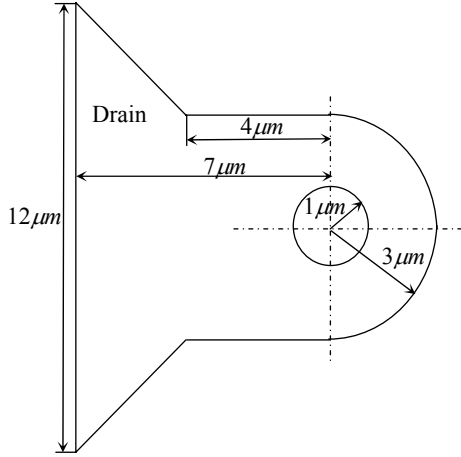


Fig. 9. The top view of the drain.

Fig. 10 is the schematic of the corresponding model used in FEA. In the model, the beam is simplified into a hemisphere with a radius of  $2 \mu\text{m}$ . We performed a rough calculation to determine whether the hemisphere is large enough. We assumed the fixed end of the beam to be at 300 K and calculated the temperature drop by conduction from the contact interface to the hemisphere boundary, and the temperature drop over that the entire beam, by calculating the corresponding thermal resistance. For a contact temperature of 500 K, the temperature at the boundary of the hemisphere would be 320K, while the assumed boundary value is 300 K. The contact is modeled as a circle of radius  $a$  shared by the beam and the drain, and multiple contact spots are not modeled. The thermal conduction of gas gaps is not included.

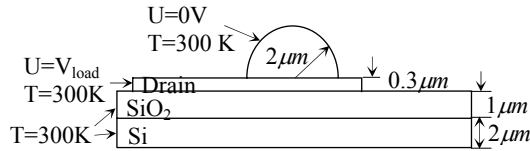


Fig. 10. FEA model in ANSYS and boundary conditions.

The geometry of the simulated drain is very similar to that in the microswitch. The thickness of the drain,  $t$ , is  $0.3 \mu\text{m}$ . The  $\text{SiO}_2$  insulating layer and the Si substrate are simplified into two cylinders. The thickness of the Si substrate was shrunk to  $2 \mu\text{m}$  to make the simulation tractable. Simulations with thicker substrates did not show any change in the thermal behavior of the model.

For the beam, the contact bump, and the substrates, the bulk material properties are used [18]. Since the drain is a thin film, it is no longer appropriate to use the bulk material properties from the literature. Therefore, the electrical resistivity of the drain films was obtained by electrical measurement in a tube furnace in the temperature range 300-1000 K. The thermal conductivity in the drain was calculated

using the same data and assuming that the Wiedemann-Franz law was obeyed.

All the surfaces that are exposed to air, i.e., the top and side surfaces of the drain and the exposed top surface of the  $\text{SiO}_2$  layer are defined as insulating surfaces. All the surfaces which extend beyond the model, i.e., the top surface of the beam hemisphere, the outer surfaces of  $\text{SiO}_2$  layer and Si substrate and the bottom surface of Si substrate, are constrained to be at a constant temperature (300K). A voltage,  $V_{\text{load}}$ , is applied to the end of the drain. The outer surface of the beam hemisphere is at electrical ground.

### B. Temperature Distribution Before and After Softening

The above model was simulated with a contact radius  $a = 0.1 \mu\text{m}$ , equivalent to the approximate total contact area based on mechanical modeling of the contacts and SEM micrographs of contacts after loading.

When a voltage is applied to the end of the drain, the temperature distribution in the model is as shown in Fig. 11. Fig. 12 shows a side view of the same temperature contours. Evidently, the beam behaves like a heat sink and remains close to room temperature, while the thin film drain has a much higher thermal resistance. Consequently, the hottest spot is not located at the contact center. Instead, it is in the drain,  $0.3 \mu\text{m}$  from the contact center.

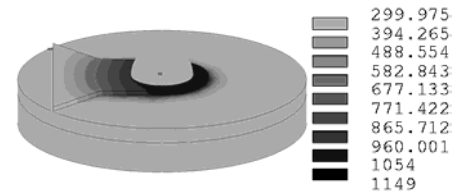


Fig. 11. Temperature contours of the microswitch model ( $V_{\text{load}}=0.35\text{V}$ ,  $a=0.1 \mu\text{m}$ , the radius of the hemisphere is  $2 \mu\text{m}$ , and the radius of substrates is  $10 \mu\text{m}$ ).

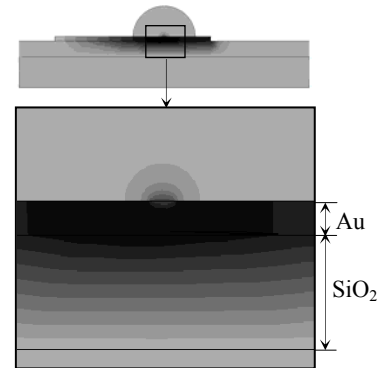


Fig. 12. Side view of Fig. 11 (The thickness of the drain metal-lization is  $0.3 \mu\text{m}$  and the thickness of the  $\text{SiO}_2$  layer is  $1.0 \mu\text{m}$ ).

If the contact is heated up to the softening temperature, the contact material will soften and the contact size will increase. To represent this situation a contact radius of  $0.5\mu\text{m}$  is used, based on electrical measurements and SEM micrographs of contacts subjected to high currents. Fig. 13 and Fig. 14 show the temperature contours for this case. The hottest spot is in the drain, about  $2.7\mu\text{m}$  from the contact – that is, further away from the contact compared to the location of the hottest spot with a  $0.1\mu\text{m}$  contact.

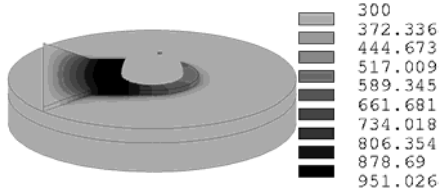


Fig. 13. Temperature contours of the microswitch model in ANSYS ( $V_{\text{load}}=0.35\text{V}$ ,  $a=0.5\mu\text{m}$ , the radius of the upper hemisphere is  $2\mu\text{m}$ , and the radius of the overall model is  $10\mu\text{m}$ ).

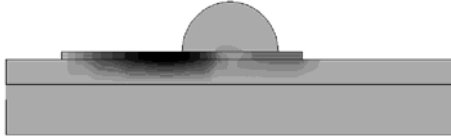


Fig. 14. Side view of Fig. 13 (The thickness of the drain metallization is  $0.3\mu\text{m}$  and the thickness of the  $\text{SiO}_2$  layer is  $1.0\mu\text{m}$ ).

### C. Voltage Temperature Relation

The voltage-temperature relation for this model was obtained from a number of simulations at different applied voltages at contact radii of  $0.1$  and  $0.5\mu\text{m}$ , and is shown in Fig. 15. The analytical expression of (2) is shown for comparison. The simulated maximum temperature is 5-10% smaller than the analytical value based on the Wiedemann-Franz law. The difference exists because the heat is lost through the electrically insulating but thermally conducting substrate.

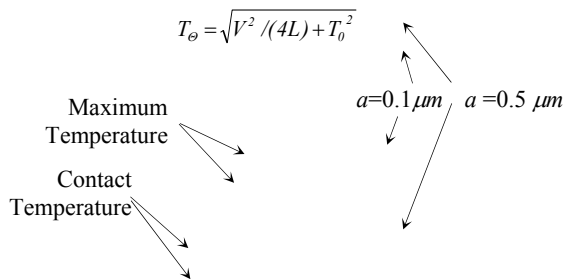


Fig. 15. Voltage temperature relation from modeling.

## V. EXPERIMENTAL RESULTS

### A. Description of Experiments

The resistance of the microswitch was measured as a function of the current through the contact. The experimental setup is shown in Fig. 16. A voltage is applied between the drain and the source terminals, and the voltage between the sense terminals is measured. The switch resistance,  $R_{\text{switch}}$ , and the switch voltage,  $V_{\text{switch}}$ , are measured while increasing the current through the switch.

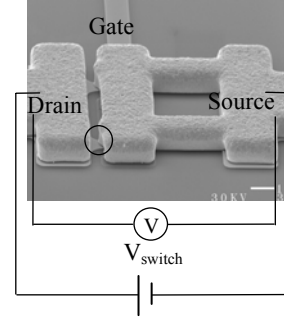


Fig. 16. Experiment setup (only the circled part is modeled in ANSYS).

### B. Experimental Results of Microswitches with Au-Au Contact

Fig. 17 shows the microswitch resistance for one contact (twice the switch resistance) as a function of switch voltage for Au-Au switches, measured at a single contact force of approximately  $30\mu\text{N}$ . The switches were kept closed during the measurement. Based on a simple clean-metal contact resistance model, the expected resistance is about  $0.2\text{-}0.6\Omega$  per contact, depending on the assumed surface roughness.

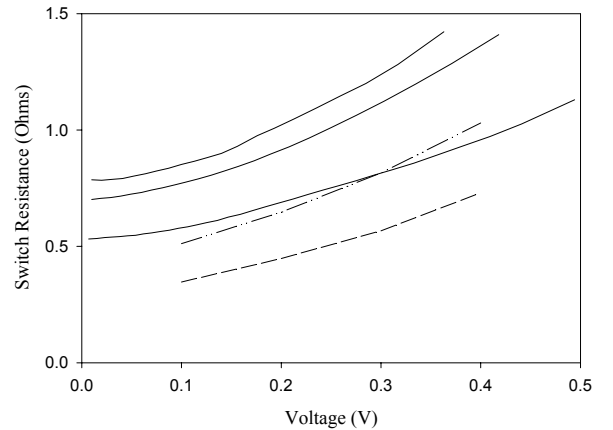


Fig. 17. Experimental results for gold/gold contact (The solid lines are experimental results; the dash-dot-dot line is from  $0.1\mu\text{m}$  contact radius model; the short-dashed line is from  $0.5\mu\text{m}$  contact radius model).

The measured resistance typically increases with increasing voltage. When the current per contact reaches 0.35A and the switch voltage reaches 0.45V, the drain thin film melts (Fig. 18). The region of maximum damage due to melting is 3-5  $\mu\text{m}$  from the center of the contact. The model predicts that the hottest spot in the drain reaches the melting point of gold when the voltage is about 0.43 V, and the hottest point is predicted to be about 2.7  $\mu\text{m}$  from the center of the contact.

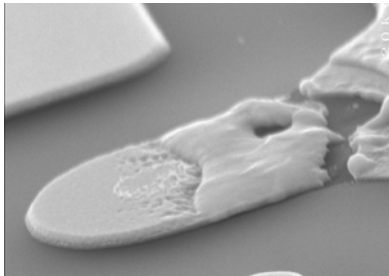


Fig. 18. Micrograph of the drain of a failed microswitch.

## VI. SUMMARY

We have developed a finite element thermal model of a micromechanical switch, in order to study its current handling capability. The model shows that the highest temperature is located very close to the contact center and within the region of contact when the contact radius is 0.1  $\mu\text{m}$ . However, if a contact radius of 0.5  $\mu\text{m}$  is assumed in order to account for softening of the contact surfaces, the hottest spot moves away from the contact into the drain trace.

Contact resistance measurements show that the switch resistance increases with voltage. At a switch current of 0.35A per contact and a voltage of 0.45V, the drain metal melts, confirming that the hottest region is not at the contact, but in the drain, 3-5  $\mu\text{m}$  from the contact. The location of the melted region is slightly further from the contact than is predicted by the model.

## ACKNOWLEDGMENT

We would like to thank Analog Devices for their support of the microswitch program at Northeastern University. We would also like to acknowledge the valuable contribution of Weilin Hu and Rick Morrison in the fabrication of the devices.

## REFERENCE

- [1] P. M. Zavracky, S. Majumder, and N. E. McGruer, "Micromechanical switches fabricated using nickel surface micromachining," *Journal of Microelectromechanical Systems*, Vol. 6, no. 1, pp. 3-9, 1997.
- [2] S. Majumder, N. E. McGruer, P. M. Zavracky, G. G. Adams, R. H. Morrison, and J. Krim, "Measurement and modeling of surface micromachined, electrostatically actuated microswitches", in *Transducers '97* (Chicago, IL, June 16-19, 1997, pp. 1145-1148).
- [3] S. Majumder, P. M. Zavracky, and N. E. McGruer, "Electrostatically actuated micromechanical switches", *Journal of Vacuum Science and Technology A*, vol. 15, no. 3, pp. 1246-1249, 1997.
- [4] J. H. Heasley, "Transient heat flow between contacting solids", *International Journal of Heat Transfer*, vol. 8, pp. 147-154, 1965.
- [5] G. E. Schneider, A. B. Stroing and M. M. Yovanovich, "Transient thermal response of two bodies communicating through a small circular contact area", *Internal Journal of Heat Transfer*, vol. 20, pp. 301-308, 1977.
- [6] S. S. Sadhal, "Unsteady heat flow between solids with partially contacting interface", *Transactions of the ASME: Journal of Heat Transfer*, vol. 103, pp. 32-35, 1982.
- [7] Seik Oh and M. D. Bryant, "The transient temperature fields for two contacting bodies having different electric potentials", *IEEE Transactions on Components: Hybrids and Manufacturing Technology*, vol. 9, no. 1, pp. 71-76, 1986.
- [8] L. S. Fletcher, "Recent developments in contact conductance heat transfer", *Transactions of the ASME: Journal of Heat Transfer*, vol. 110, pp. 1059-1070, 1988.
- [9] T. S. Davies, H. Nouri and M. Fairhurst, "Experimental and theoretical study of heat transfer in switches", in *Proceedings of 42<sup>nd</sup> IEEE Holm Conf. on Electrical Contacts* ( Chicago, IL, Sep 16-20, 1996, pp. 45-49).
- [10] Chi. H. Leung, Anthony Lee, Bor-Jenq Wang, "Contacts in switches and relays", *IEEE Transactions on Components, Packaging, and Manufacturing Technology A*, vol. 19, no. 3, pp. 346-352, 1996.
- [11] Daniel Hyman and Mehran Mehregany, "Contact physics of gold microcontacts for MEMS switches", in *Proc. of 44<sup>th</sup> IEEE Holm Conf. on Electrical Contacts* (Arlington, VA, October 26-28, 1998, pp.133-140).
- [12] R. Holm, *Electric Contacts: Theory and Application*, New York: Springer-Verlag, 1967.
- [13] S. Majumder, N. E. McGruer, "Study of contacts in an electrostatically actuated microswitch", in *Proc. of 44<sup>th</sup> IEEE Holm Conf. on Electrical Contacts* (Arlington, VA, October 26-28, 1998, pp.127-132).
- [14] J. A. Greenwood, and J. B. P. Williamson, "Contact of nominally flat surfaces", *Proc. Roy. Soc. A*, vol. 295, pp. 300-319, 1966.
- [15] W. R. Chang, I. Etsion, and D. B. Bogy, "An elastic-plastic model for the contact of rough surfaces", *Journal of Tribology*, vol. 109, no. 2, pp. 257-263, 1987.
- [16] P. Bowden, F. R. S and J. B. P. Williamson, "Electrical conduction in solids I: Influence of the passage of current on the contact between solids", *Proc. Roy. Soc. A*, vol. A246, pp. 1-12, 1958.
- [17] J. A. Greenwood, and J. B. P. Williamson, "Electrical conduction in solids II: Theory of temperature-dependent conductors", *Proc. Roy. Soc. A*, vol. A246, pp. 13-31, 1958.
- [18] V. E. Vlad Zinovev, *Handbook of Thermophysical Properties of Metals*, New York: Nova Science Publishers, 1996.